Thin Solid Films 549 (2013) 36–41

Contents lists available at ScienceDirect

Thin Solid Films

journal homepage: www.elsevier.com/locate/tsf

Investigation on plasma treatment for transparent Al–Zn–Sn–O thin film transistor application

Chih-Hsiang Chang [a], Po-Tsun Liu [b,*]

[a] Department of Photonics & Institute of Electro-Optical Engineering, National Chiao Tung University, Hsinchu, 30010, Taiwan, ROC
[b] Department of Photonics & Display Institute, National Chiao Tung University, Hsinchu, 30010, Taiwan, ROC

ARTICLE INFO

Available online 4 July 2013

Keywords:
Thermal annealing
AlZnSnO TFT
Plasma post treatment
Oxygen bonding
Reliability mechanism

ABSTRACT

This work reported the physical characteristics and electrical performance of amorphous Al–Zn–Sn–O thin film transistor (a-AZTO TFT) device under the temperature effects of thermal annealing process and various gas plasma post-treatments. The thermal annealing at 450 °C could strengthen the oxygen bonding of a-AZTO film, thereby improving the film quality and TFT device performance. In addition, the oxygen deficient can be reduced effectively by the O_2 and N_2O plasma treatments, respectively, leading to enhanced electrical reliability. Also, the optical energy gap of a-AZTO films with O_2 or N_2O plasma treatment was measured about 3.5 eV, which indicated that all of the a-AZTO films were insensitive to visible light. On the other hand, the electron mobility of a-AZTO TFT was observed to be promoted after NH_3 plasma post-treatment. The improvement could be attributed to a slight doping effect of H^+ ions. These results showed the potential of post-treatments for flat panel displays applications of transparent a-AZTO TFT technology.

1. Introduction

In recent years, thin film transistors (TFTs) using transparent amorphous oxide semiconductor (TAOS) as a display backplane technology have attracted a lot of attention for large-sized liquid-crystal displays and active-matrix organic light-emitting diode displays. Many candidates of transparent oxide TFTs have been widely studied by using In–Zn–O [1], Si–In–Zn–O [2], Hf–In–Zn–O [3], and In–Ga–Zn–O [4] as the active channel layer, owing to their characteristics of low-power consumption, high-speed operation, high-density integration, and high process compatibility with the present flat-panel display industry [5–7]. Although these proposed oxide TFT devices showed good electrical performance, the large use of rare-dispersive elements, such as In and Ga, has been a critical issue for the long-term technology applications. Therefore, rare elements-free oxide semiconductors are considered to be the promising candidates for the next generation display device technologies. In this paper, Al–Zn–Sn–O (AZTO) semiconductor material is studied for active channel layer of TFT device. All components in AZTO thin film are rich and common in the Earth. For practical operation in FPD applications, it is necessary for the electronic devices to exhibit a good immunity against the reliability issues known as gate bias stress (GBS) and photo-induced stress. Even though some literatures showed that the amorphous AZTO TFT (a-AZTO TFTs) could deposit at room temperature and exhibit good electrical performance and reliability [8], the study of physical characteristic and operation mechanisms is still lacking. In this study, the effects of thermal annealing and plasma post-treatment processes are studied in detail. Physical mechanisms for the enhancement of electrical and photosensitive reliability are also proposed through the analyses of electrical characteristics and X-ray photoelectron spectroscopy (XPS).

2. Experiment

In this work, bottom gate inverted staggered TFT devices using a-AZTO film as a channel layer was studied. At first, a layer of 100-nm-thick silicon dioxide was thermally grown on n-type silicon wafers. The a-AZTO films were then deposited by radio-frequency (RF) magnetron sputtering using an AZTO ceramic plate target that consisted of ZnO, SnO_2 and Al_2O_3 (47: 50: 3 mol %). Ar gas flow rate was set to 10 sccm, and the O_2 flow rate was set to 2 sccm, and the sputtering pressure and power were 3 mTorr and 80 W, respectively, at room temperature. A layer of 100 nm-thick indium tin oxide film was deposited subsequently by the RF sputtering, and patterned through a shadow mask as source and drain (S/D) electrodes. The channel width and length ranged from 200 um to 1000 um, and the width/length ratio were set from 0.2 to 5. The cross-sectional view of a-AZTO TFT device structure is illustrated schematically in Fig. 1. The a-AZTO TFT devices were thermally annealed ranging from 350 °C to 450 °C for 60 min by a thermal furnace in the nitrogen atmosphere for defect elimination. Another group of TFT devices after thermal annealing process was post-treated by O_2 plasma, N_2O plasma, NH_3 plasma, respectively, to passivate the defects in a-AZTO

* Corresponding author at: Department of Photonics and Display Institute, National Chiao Tung University, CPT Building, Room 412, 1001 Ta-Hsueh Rd. Hsin-Chu 300, Taiwan, ROC. Tel.: +886 3 5712121x52994; fax: +886 3 5735601.
E-mail address: ptliu@mail.nctu.edu.tw (P.-T. Liu).

0040-6090/$ – see front matter
http://dx.doi.org/10.1016/j.tsf.2013.06.042

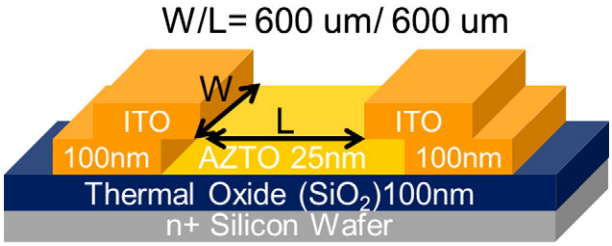

Fig. 1. a-AZTO TFT device structure.

film. All electrical measurements were carried out at a semiconductor parameter analyzer, Keithley 4200.

3. Result and discussions

Fig. 2 shows intrinsic electrical characteristics of a-AZTO TFT devices with different thermal annealing temperatures at 350 °C, 400 °C, and 450 °C. Error bar in Fig. 2 (b) presents the difference between devices in the same process conditions. Its observed threshold voltage was negatively shifted from 12.05 to 2.42 V, while the mobility increased from 0.15 to 5.58 $cm^2/V\,s$ as the annealing temperature increased. The improvement in TFT device performance can be attributed to an enough annealing temperature, which led to the lattice structure rearrangement and structural relaxation of a-AZTO bonding.

XPS analysis was conducted to observe the relationship of oxygen bonding and annealing temperatures. After different thermal annealing processes, there was no obvious change in the signal peaks of elements of Al, Zn and Sn (not shown), while the significant change of oxygen (O 1 s) peak was observed as shown in Fig. 3. The O

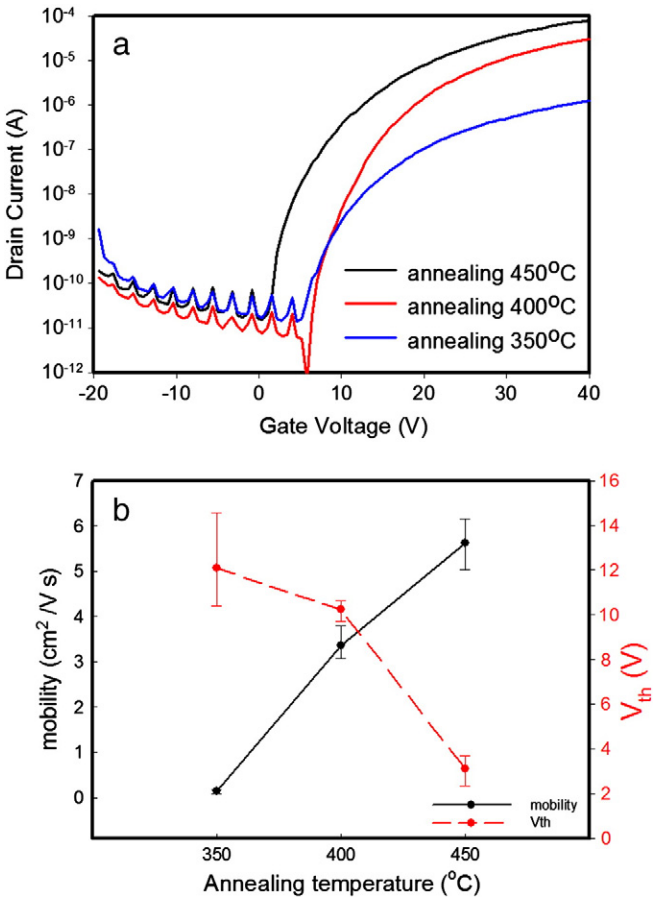

Fig. 2. The immediate comparison of I_D-V_G of a-AZTO TFT with different annealing temperature. (b) The device parameters' error bar with different annealing temperature. Each error bar includes five different measuring results for each TFT devices.

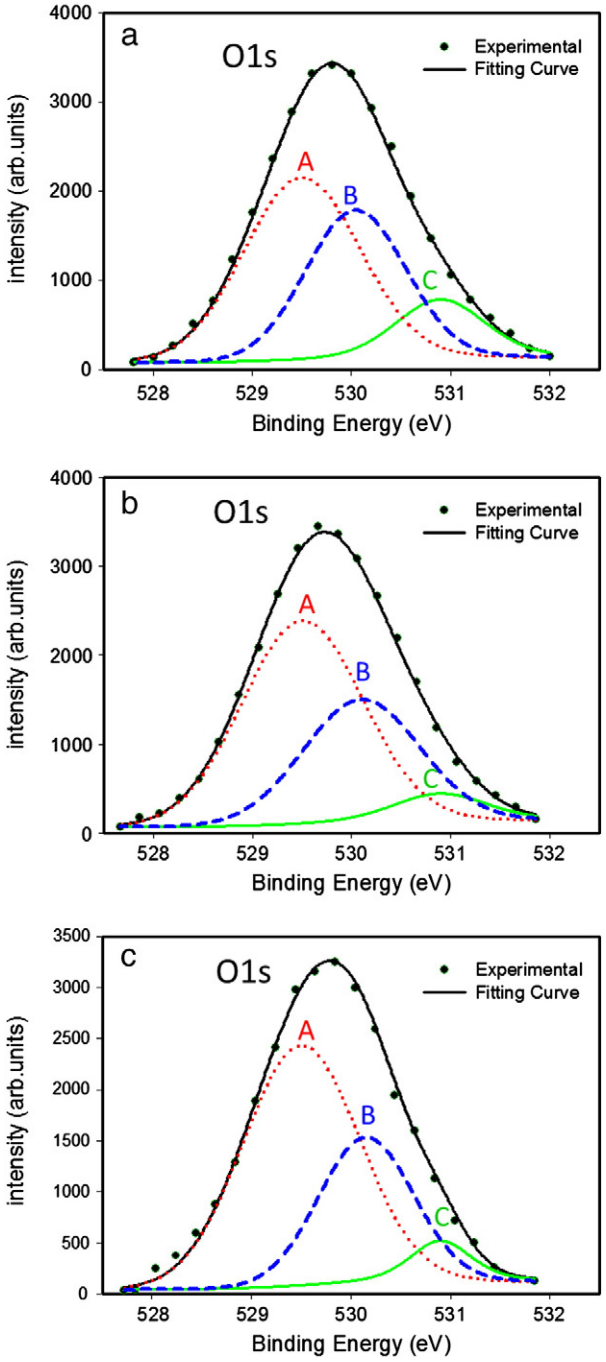

Fig. 3. XPS analyses of O 1 s spectra for the a-AZTO thin films with furnace annealing at (a) 350 °C, (b) 400 °C, and (c) 450 °C, respectively. Peak A denotes the lowering binding peak centered at 529.5 eV, generated from the lattice oxygen ions with neighboring metal atoms. Peak B is the higher binding energy peak at 530.1 eV corresponding to O^{2-} ion at oxygen-deficient region with the matrix of the a-AZTO film. Peak C stands for the oxygen desorption or OH^- impurities which centers at 530.9 eV.

1 s peaks centered at binding energies of 529.5 eV, 530.1 eV, and 530.9 eV are related to oxygen in oxide lattices without oxygen vacancies (oxygen binding), with oxygen deficient, and with OH^- impurities, respectively [9]. It can be clearly seen that the relative area of the oxygen-deficient-related peak decreased as the annealing temperature increased. The values are 35.6%, 34.3% and 30.8% for the annealing temperature at 350 °C, 400 °C, and 450 °C, respectively. It meant the better oxidized stoichiometry was obtained through the increase of annealing temperatures.

Compared with the a-AZTO TFT without any plasma treatment, the threshold voltage shift of O_2 and N_2O plasma-treated ones under positive and negative GBS is shown in Fig. 4 (a) and (b), respectively. The threshold voltage shift ($\triangle V_{th}$) was defined as the variation of threshold voltage value before and after GBS process. It is clearly observed $\triangle V_{th}$ was decreased for the plasma-treated a-AZTO TFT devices. Fig. 5 shows XPS O 1 s peaks of a-AZTO films with O_2 and N_2O plasma post treatment, respectively, in comparison with the one without any plasma treatment. The relative area of the oxygen-deficient-related peak decreased after O_2 and N_2O plasma post treatment. The values are 32.3%, 27.7% and 25.1% for the samples without plasma treatment, with O_2 plasma, and with N_2O plasma treatment, respectively. O_2 and N_2O plasma post treatment could enhance oxidizing the a-AZTO film so that it strengthened oxygen atomic bonding and decreased the density of oxygen vacancies and the oxygen-related trap states. As a result, the electrical reliability of TFT devices with O_2 and N_2O plasma post treatment was obviously improved after being subjected to PGBS and NGBS testing.

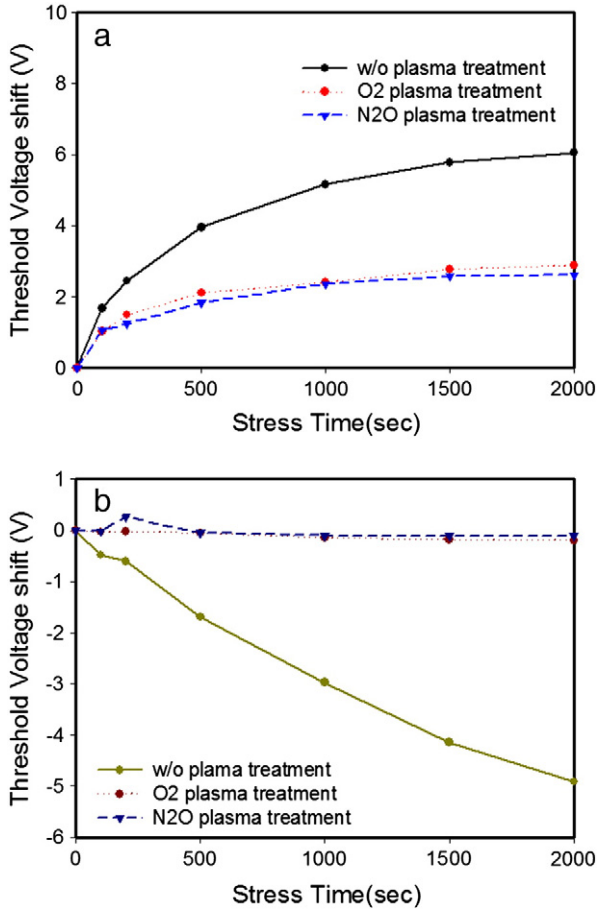

Fig. 4. Threshold voltage shift under (a) positive and (b) negative gate bias stress (GBS) with O_2, N_2O plasma post-treatment, and the reference sample (w/o plasma treatment). The gate bias stress conditions were 2.5 MV/cm for positive bias and −2.5 MV/cm for negative bias stress at room temperature for 2000 s, while source and drain electrodes connected to ground.

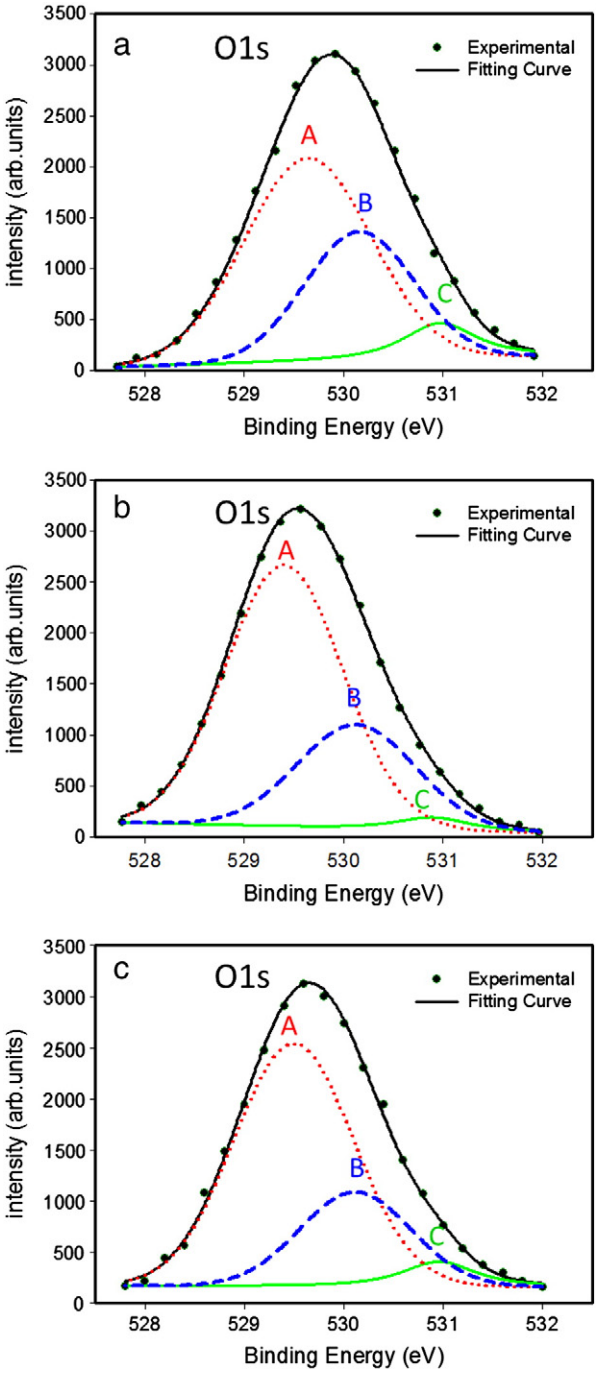

Fig. 5. XPS analyses of O 1 s spectra for the a-AZTO thin films with furnace annealing at 450 °C and (a) w/o plasma treatment, (b) O_2 plasma treatment, and (c) N_2O plasma treatment, respectively. Peak A denotes the lowering binding peak centered at 529.5 eV, generated from the lattice oxygen ions with neighboring metal atoms. Peak B is the higher binding energy peak at 530.1 eV corresponding to O^{2-} ion at oxygen-deficient region with the matrix of the a-AZTO film. Peak C stands for the oxygen desorption or OH^- impurities which centers at 530.9 eV.

Fig. 6 (a) shows the transparency of a-AZTO film through the visible spectrum analysis. The transmittance for all samples is greater than 80% with the wavelengths ranging from 400 nm to 700 nm. Also, this means that O_2 or N_2O plasma post treatment was not degrading the transparency of a-AZTO film. It is well known that the optical transparency of dielectric materials is proportional to their optical band-gap (E_g), which can be theoretically obtained according to

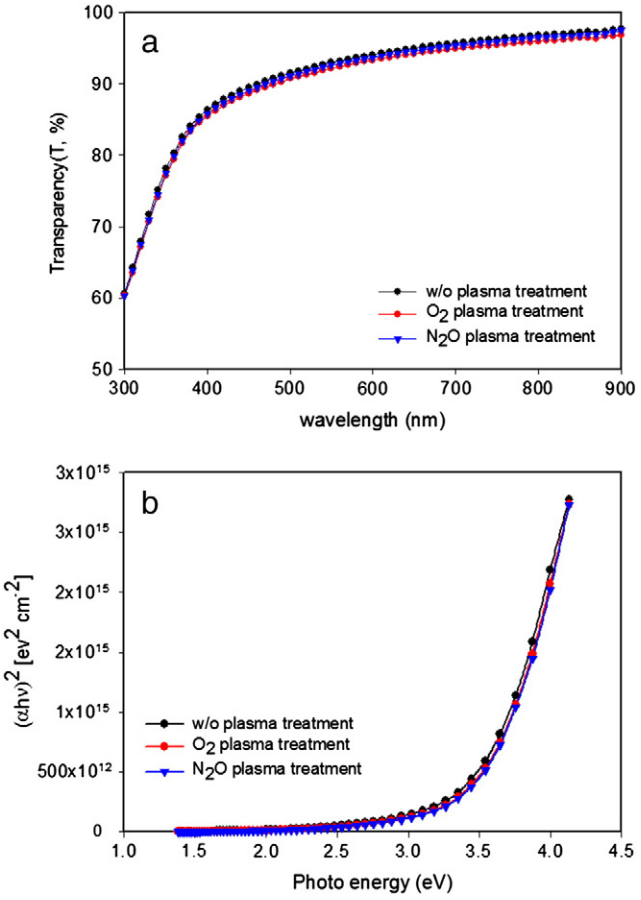

Fig. 6. (a) The transmittance of a-AZTO film with O_2 and N_2O plasma post-treatment versus different wavelength lights. (b) The plot of $(\alpha h\nu)^2$ versus photo energy ($h\nu$) following Tauc model and Davis and Mott model.

Tauc model [10], and the Davis and Mott model in the high absorbance region, as followed:

$$(\alpha h\nu)^n = D * \left(h\nu - E_g\right)$$

where α is the absorption coefficient, $h\nu$ the photon energy, Eg the optical band gap, and D is a constant. The constant n is usually equal to 2 for amorphous semiconductors since it gives the best linear curve in the band-edge region.

The relationships between $(\alpha h\nu)^2$ and the photon energy ($h\nu$) are characterized for a-AZTO films with O_2 and N_2O plasma post treatment, as shown in Fig. 6b. The absorption coefficient α can be obtained from the transmittance data by using the equation of $\alpha = (1/d)^* \ln(1/T)$, where d and T are the thickness and the transmittance of the a-AZTO films with O_2 and N_2O plasma post treatment, respectively. The optical band-gaps, Eg, can be obtained by extrapolating from the linear region onto the axis of photon energy, as shown in Fig. 6 (b). The obtained values of optical band-gaps for the -AZTO films with O_2 and N_2O plasma post treatment are summarized in Table 1. There is no large difference in the optical band-gaps of all a-AZTO films.

Table 1
Band-gap energy for different plasma treated a-AZTO thin film.

	Without any plasma treated	O_2 plasma 50 s	N_2O plasma 50 s
Band-gap energy (eV)	3.50	3.54	3.55

The negative bias illumination stress (NBIS)-induced instability of the electrical properties of a-AZTO TFT devices was also investigated in this study, as shown in Fig. 7. In this stress testing, the gate voltage (V_G) was fixed at −25 V and the S/D electrodes were grounded under the green light with energy of 2.27 eV and blue light illumination with energy of 2.85 eV for 2000 s, respectively. Fig. 7a shows the a-AZTO TFT without any plasma treatment exhibited a negative threshold voltage shift about −5.5 V, while almost no electrical degradation was observed during the testing of negative bias and green light illumination (NBGIS). As reported by Nomura et al. [11], the high density of occupied subgap states existed in the energy gap of TAOS near the valence band width with an energy width of ~1.5 eV. The increase of free carrier concentration in the a-AZTO films can occur due to the light illumination offering enough photo-energy larger than 1.7 eV to induce carrier excitation from the deep-subgap density of state to the conduction band [12]. Besides, a negative bias was applied with light illumination, resulting in the V_o^{2+} trapping in the insulator or a-AZTO/gate insulator interface [13]. Both of the results contribute to the apparent threshold voltage shift under NBIS. Compared with NBGIS, TFT device without plasma post treatment exhibited a large photo-induced leakage current during the negative bias with blue light illumination stress (NBBIS), which induced a negative threshold voltage shift about −6.3 V, as shown in Fig. 7 (a) and (b). This result indicated that the threshold voltage shift increased gradually as the light photo-energy increased during NBIS for the device without plasma treatment. Fig. 7 (c) and (d) shows the corresponding threshold voltage variation of all the TFT devices after being subjected to NBGIS and NBBIS, respectively. The a-AZTO TFT with O_2 or N_2O plasma treatment shows a significantly low threshold voltage shift (ΔV_{th} ~ 0.1 V) than that without plasma treatment. The reliability improvement can be attributed to the reduction of deep trap density, leading to relax the photo-induced excitation behavior.

According to previous literature, it reported that the H atoms always form O–H bonds by DFT structure relaxation calculations [13]. This indicates that the H doping results in electron doping through the reaction H (from ambient) + O^{2-} (in a-IGZO)→ –OH (in a-IGZO) + e^-. A similar effect was also reported for ZnO [14,15]. The H doping would be strong and stable because the doped H atoms form strong O–H bonds. In this work, NH_3 plasma post-treatment was proposed to study the effect of H doping on a-AZTO TFT characteristics. The transfer curve of NH_3 plasma-treated a-AZTO TFT is compared with the one without plasma treatment, as shown in Fig. 8 (a) and (b). The threshold voltage decreased from the 6.1 V to about −0.1 V after NH_3 plasma post treatment. The electron mobility slightly increased from 3.8 cm^2/V s to 3.9 cm^2/V s and 4.0 cm^2/V s, respectively, for the NH_3 plasma treatment duration of 50 sec and 200 sec. According to the XPS O 1 s peaks shown in Fig. 9 (a), (b), and (c), the relative area of oxygen-hydrogen bonding in a-AZTO thin film increased from 6.8% to 9.8% after NH_3 plasma treatment 200 s. As reported by the previous literature, hydrogen atoms doped to a-IGZO model potentially forms –OH bonds. The stable O–H bonds are formed when three cations (Zn–O, In–O, Zn–O) are bonded to the oxygen ion in the O-H bond, while if only two cations (Ga–O, Ga–O) are bonded to the oxygen ion in the O–H bond, E_{form} are large and such O–H bonds are hardly created [16]. Since Ga–O is the strongest bond among the constituent chemical bonds in a-IGZO, the O–H bonds are easily formed at the oxygen deficiency site.

Based on above-mentioned results regarding the effect of thermal annealing temperature, the oxygen deficient increased as the annealing temperature decreases. A combination of NH_3 plasma

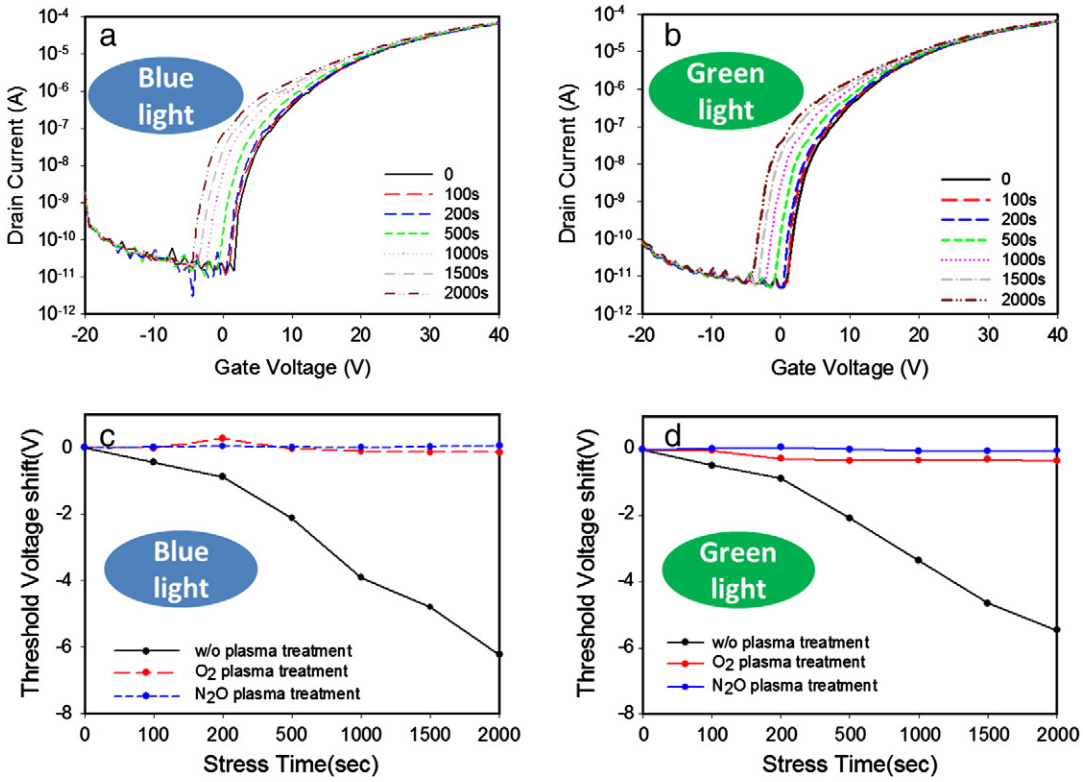

Fig. 7. Transfer I–V characteristics for the device without plasma post-treatment during the negative bias illumination stress (NBIS) of (a) blue (b) green lights. Threshold voltage shift of negative bias light illumination stress (NBIS) of (c) blue (d) greens lights for a-AZTO TFTs with and without plasma post-treatment.

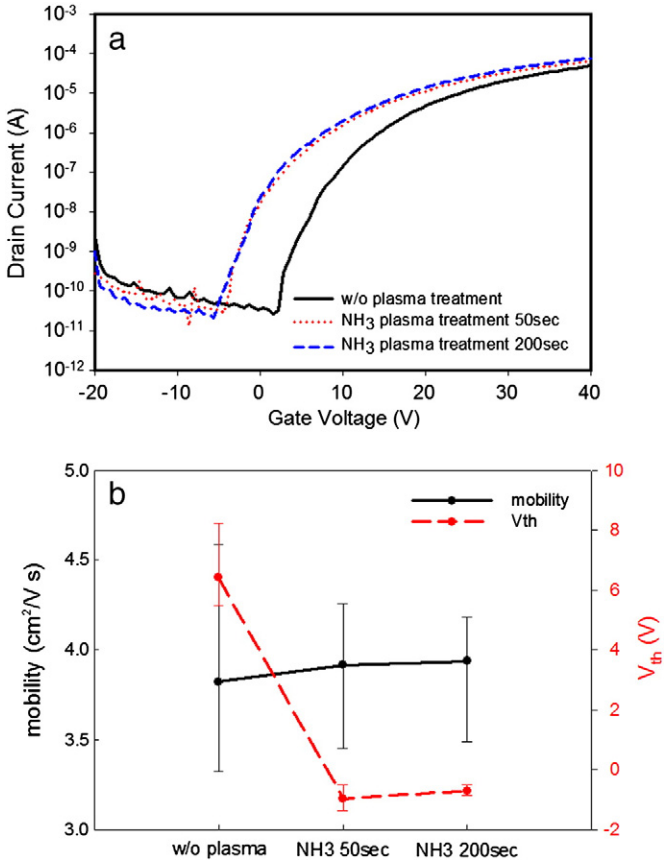

Fig. 8. (a) The transfer characteristics of a-AZTO TFT under 450 °C annealing process adds NH_3 plasma post-treatment 50 s, 200 s and reference (b) the device parameters' error bar with NH_3 plasma treatment 50 s, 200 s and reference. Each error bar includes five different measuring results for each TFT devices.

treatment and lower-temperature thermal annealing was proposed to develop a low-temperature fabrication of a-AZTO TFT with improved electrical performance. Fig. 10 shows the transfer characteristics of 350 °C-annealed a-ATZO TFT devices with NH_3 plasma post-treatments for different durations. Compared with the 350 °C-annealed TFT without NH_3 plasma, threshold voltage shifted negatively from +11 V to about +6.5 V after NH_3 plasma post-treatment. On the other hand, the electron mobility increases from 0.5 cm^2/V s to 1.1 cm^2/V s and 1.2 cm^2/V s, respectively, for NH_3 plasma treatment duration of 50 s and 200 s. In other words, the electron mobility enhanced above 130% after NH_3 plasma post-treatment. In short, we can effectively promote the conductivity of low-temperature annealed a-AZTO thin films with NH_3 plasma treatment.

4. Conclusions

The physical characteristic and electrical performance of a-AZTO TFTs with different annealing temperatures and plasma post-treatments have been discussed in this work. The higher annealing temperature can strengthen the oxygen bonding in a-AZTO layer, and thereby the electrical performance of TFT device is effectively enhanced. Moreover, O_2 and N_2O plasma can oxidize the a-AZTO film and eliminate some of the oxygen deficients. As a result, the reliability of the devices under GBS improves significantly after O_2 and N_2O plasma post-treatment. The optical energy gap of a-AZTO films with O_2 or N_2O plasma treatment are about 3.5 eV which indicated that the a-AZTO film is insensitive to visible light. On the other hand, NH_3 plasma post-treatment can release H^+ ions into the a-AZTO thin film and increase the conductivity of the thin film as well. A low-temperature annealing process of a-AZTO TFT fabrication was successfully developed to enhance electron mobility by associating with NH_3 plasma post-treatment.

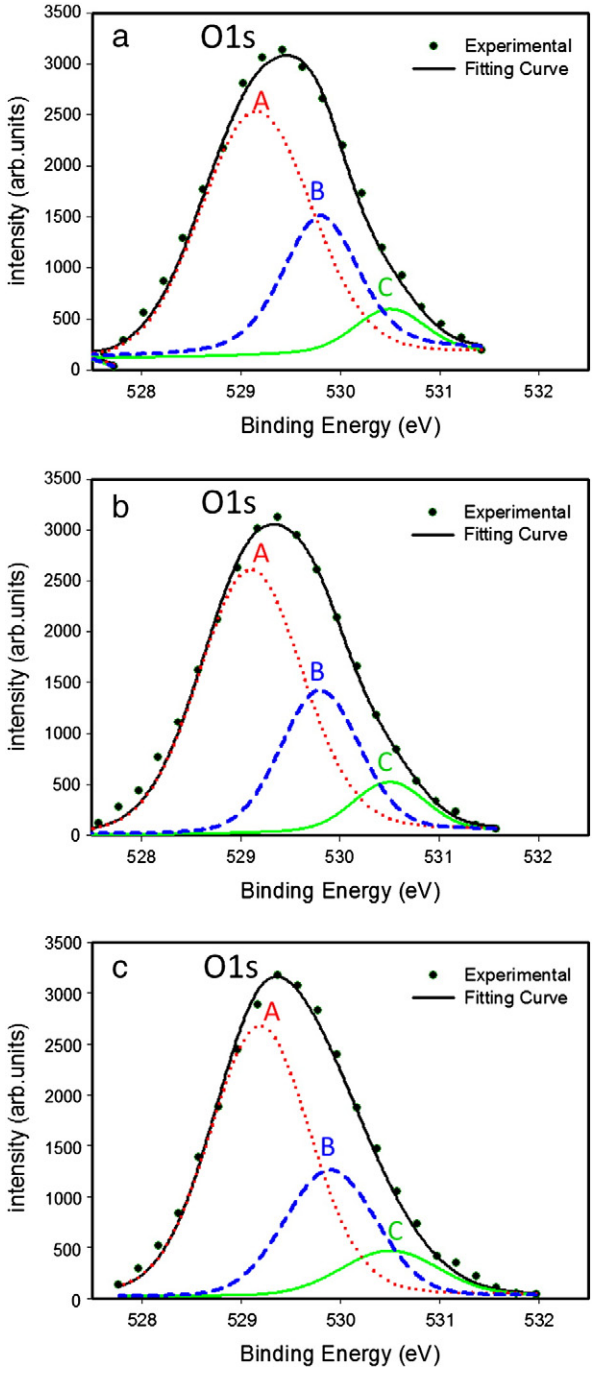

Fig. 9. XPS analyses of O 1 s spectra for the a-AZTO thin films with furnace annealing at 450 °C and (a) w/o plasma treatment, (b) NH_3 plasma treatment for 50 seconds, and (c) NH_3 plasma treatment for 200 s, respectively. Peak A denotes the lowering binding peak centered at 529.5 eV, generated from the lattice oxygen ions with neighboring metal atoms. Peak B is the higher binding energy peak at 530.1 eV corresponding to O^{2-} ion at oxygen-deficient region with the matrix of the a-AZTO film. Peak C stands for the oxygen desorption or OH^- impurities which centers at 530.9 eV.

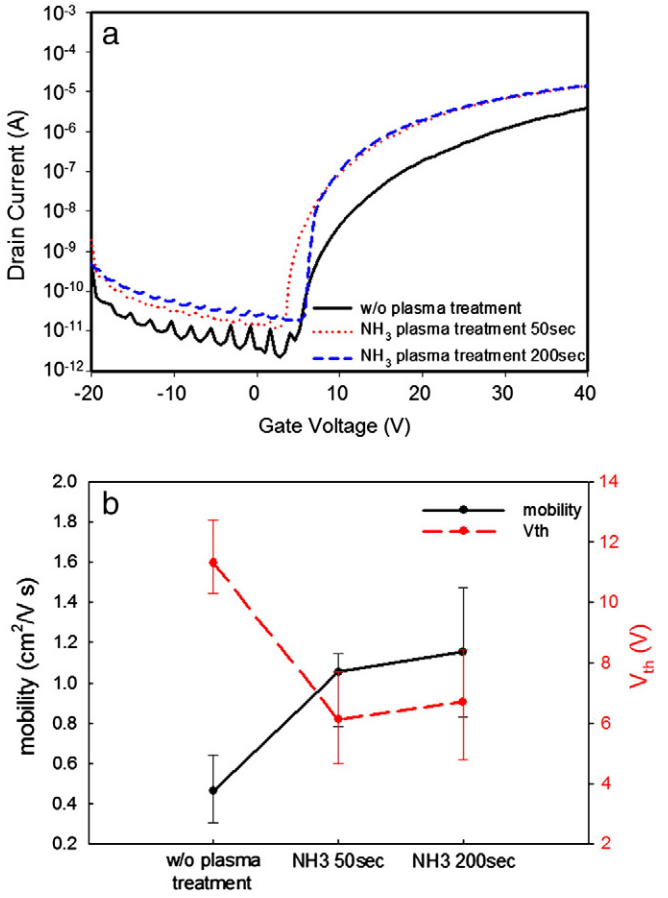

Fig. 10. (a) The transfer characteristics of a-AZTO TFT under 350 °C annealing process adds NH_3 plasma post-treatment 50 s, 200 s and reference (b) the device parameters' error bar with NH_3 plasma treatment 50 s, 200 s and reference. Each error bar includes five different measuring results for each TFT devices.

Acknowledgement

The authors would like to thank the National Science Council of the Republic of China, Taiwan for financially supporting this research under Contract No. NSC 100-2628-E-009-016. Also, this work was performed at the National Nano Device Laboratories, Taiwan, ROC.

References

[1] P.T. Liu, Y.T. Chou, L.F. Teng, Appl. Phys. Lett. 95 (2009) 233504.
[2] E. Chong, Y.S. Chun, S.Y. Lee, Appl. Phys. Lett. 97 (2010) 102102.
[3] S.J. Kim, S.Y. Lee, Y.W. Lee, W.G. Lee, K.S. Yoon, J.Y. Kwon, M.K. Han, Jpn. J. Appl. Phys. 50 (2011) 024104.
[4] M. Kim, J.H. Jeong, H.J. Lee, T. K.g Ahn, H.S. Shin, J.S. Park, J.K. Jeong, Y.G. Mo, H.D. Kim, Appl. Phys. Lett. 90 (2007) 212114.
[5] K. Nomura, H. Ohta, A. Takaji, T. Kamlya, M. Hirano, H. Hosono, Nature 432 (2004) 488.
[6] J.S. Park, K.S. Kim, Y.G. Park, Y.G. Mo, Adv. Mater. 21 (2009) 329.
[7] C.J. Chiu, S.P. Chang, S.J. Chang, IEEE Electron Device Lett. 31 (2010) 1245.
[8] D.H. Cho, S. Yang, C. Byun, J. Shin, M.K. Ryu, S.H. Ko Park, C.S. Hwang, S.M. Chung, W.S. Cheong, S.M. Yoon, H.Y. Chu, Appl. Phys. Lett. 9 (2008) 1421113.
[9] S. Yang, K.H. Ji, Un Ki Kim, C.S. Hwang, S.H. Ko Park, Appl. Phys. Lett. 99 (2011) 102103.
[10] E.A. Davis, N.F. Mott, Philos. Mag. 22 (1970) 903.
[11] K. Nomura, T. Kamiya, H. Yanagi, E. Ikenaga, K. Yang, K. Kobayashi, M. Hirano, H. Hosono, Appl. Phys. Lett. 92 (2008) 202117.
[12] S. Lee, Appl. Phys. Lett. 95 (2009) 232106.
[13] T. Kamiya, K. Nomura, H. Hosono, J. Disp. Technol. 5 (12) (December 2009).
[14] C.G. Van de Walle, Phys. Rev. Lett. 85 (2000) 1012.
[15] C.G. Van de Walle, J. Neugebauer, Nature 423 (2003) 626.
[16] T. Kamiya, K. Nomura, H. Hosnos, Phys. Status Solidi A 207 (7) (2010) 1698.